UNIVERSITY OF TURKU

# AB INITIO INVESTIGATIONS OF THE DURABILITY OF IRON ALLOYS AND TITANIUM

Eero Nurmi

TURUN YLIOPISTON JULKAISUJA – ANNALES UNIVERSITATIS TURKUENSIS
SARJA - SER. AI OSA - TOM. 605 | ASTRONOMICA - CHEMICA - PHYSICA - MATHEMATICA | TURKU 2019

UNIVERSITY OF TURKU

# AB INITIO INVESTIGATIONS OF THE DURABILITY OF IRON ALLOYS AND TITANIUM

Eero Nurmi

TURUN YLIOPISTON JULKAISUJA – ANNALES UNIVERSITATIS TURKUENSIS
SARJA - SER. AI OSA - TOM. 605 | ASTRONOMICA - CHEMICA - PHYSICA – MATHEMATICA | TURKU 2019

**University of Turku**

Faculty of Science and Engineering
Department of Physics and Astronomy

## Supervised by

Professor Kalevi Kokko
Department of Physics and Astronomy
University of Turku
Turku, Finland

## Reviewed by

Professor Kari Laasonen
Department of Chemistry and Materials Science
Aalto University
Espoo, Finland

Professor Pär Olsson
Head of Nuclear Engineering
Director of doctoral program in physics
KTH Royal Institute of Technology
Stockholm, Sweden

## Opponent

Professor Tapio Rantala
Department of Physics
Tampere University
Tampere, Finland



ISBN 978-951-29-7637-9 (PRINT)
ISBN 978-951-29-7638-6 (PDF)
ISSN 0082-7002 (Print)
ISSN 2343-3175 (Online)
T. Nieminen Oy Painotalo Painola – Piispanristi, Finland 2019

# Acknowledgments

This has been a long journey. There have been moments when it seemed improbable for this dissertation to ever be finished. However, the final form of this thesis was gradually achieved. There are several people and organizations that I would like to acknowledge for that.

I would like to express my sincere gratitude to my supervisor Professor Kalevi Kokko. The completion of this work would not have been possible without his support, guidance and patience. I also wish to thank Professor Levente Vitos for sharing the EMTO calculation program and helping with his unparalleled knowledge of the calculation method and physics behind it. I would like to thank Graduate School of Materials Research (GSMR) and National Doctoral Programme in Nanoscience (NGS-NANO) for the financial support. For the computer resources I would like to acknowledge the Finnish IT Center for science (CSC) and Mgrid project.

I gratefully acknowledge the colleagues, friends and all the others who have helped or encouraged me in during this work. I am grateful to my parents and my brothers for the inspiring childhood and youth. Finally, I would like to thank my wife Viivi for being loving and supportive, and my daughter Sofia for bringing joy to my life and being an excellent reason to finish this thesis.

# Abstract

In this *ab initio* work the oxidation of Fe-Cr, Fe-Al, Fe-Cr-V and Fe-Cr-Al, and the elasticity of Fe-Cr-Al alloys and titanium were investigated. The computational method used was Exact Muffin-tin Orbitals method (EMTO). Oxidation was modelled with thermodynamic simulations of the surface composition of the investigated alloy. The elasticity of titanium and Fe-Cr-Al alloy and also the ductility of the Fe-Cr-Al alloy was simulated by calculating the total energies for deformed structures.

Corrosion resistance of iron alloys is based on the formation of the protective layers on the surface of the alloy. The addition of vanadium in Fe-Cr alloy was computationally predicted to improve the formation of the protective scales. The addition of Al increases the corrosion resistance of pure iron but impairs the mechanical properties. On the other hand, a suitable third alloying element improves the corrosion resistance. The concentration boundaries for corrosion resistance and also for ductility for Fe-Cr-Al alloys were presented. The ductility of Fe-Cr-Al was modelled with elastic constants calculations. Elastic constants calculations were also performed for pure titanium and the results were used to model the mechanical properties of cold rolled titanium.

# Tiivistelmä

Tässä väitöskirjatyössä tutkittiin kvanttifysiikan lähtökohdista, ilman kokeita simuloiden Fe-Cr, Fe-Al, Fe-Cr-V ja Fe-Cr-Al -seoksien hapettumista sekä Fe-Cr-Al-seoksen ja titaanin elastisuutta. Laskentamenetelmänä käytettiin eksaktien muffin-tin-orbitaalien menetelmää (EMTO). Hapettuminen mallinnettiin tutkittavan materiaalin pinnan koostumuksen termodynaamisilla simulaatioilla. Titaanin ja Fe-Cr-Al-seoksen elastisuutta samoin kuin Fe-Cr-Al-seoksen haurautta tutkittiin laskemalla venytettyjen rakenteiden kokonaisenergioita.

Rautaseosten korroosiokestävyys perustuu suojaavien kerrosten muodostumiseen seoksen pinnalle. Laskennallisesti ennustettiin, että vanadiinin lisäys Fe-Cr-seokseen edistää suojaavien kalvojen muodostumista. Alumiinin lisääminen puhtaaseen rautaan parantaa korroosiokestävyyttä mutta heikentää mekaanisia ominaisuuksia. Toisaalta myös sopivan kolmannen seostettavan aineen lisääminen parantaa seoksen korroosiokestävyyttä. Työssä esitetään seostettavien metallien konsentraatiorajat metallin hauraudelle ja korroosiokestävyydelle. Fe-Cr-Al-seoksen haurautta mallinnettiin laskettujen elastisten vakioiden avulla. Elastiset vakiot laskettiin myös puhtaalle titaanille ja tuloksia käytettiin kylmävalssatun titaanin mekaanisten ominaisuuksien mallintamiseen.

# List of Papers

Publications Included in the Thesis:

I Airiskallio, E., **Nurmi, E.**, Väyrynen, I. J., Kokko, K., Ropo, M., Punkkinen, M. P. J., Johansson, B., Vitos, L., "Tuning the surface chemistry of Fe-Cr by V doping", Phys. Rev. B **80**, 153403 (2009).

II Airiskallio, E., **Nurmi, E.**, Heinonen, M. H., Väyrynen, I. J., Kokko, K., Ropo, M., Punkkinen, M. P. J., Pitkänen, H., Alatalo, M., Kollár, J., Johansson, B., Vitos, L., "Third element effect in the surface zone of Fe-Cr-Al alloys", Phys. Rev. B **81**, 033105 (2010).

III Airiskallio, E., **Nurmi, E.**, Heinonen, M., Väyrynen, I., Kokko, K., Ropo, M., Punkkinen, M., Pitkänen, H., Alatalo, M., Kollár, J., Johansson, B., Vitos, L., "High temperature oxidation of Fe–Al and Fe–Cr–Al alloys: The role of Cr as a chemically active element", Corrosion Science **52**, 3394–3404 (2010).

IV Heinonen, M. H., Kokko, K., Punkkinen, M. P. J., **Nurmi, E.**, Kollár, J., Vitos, L., "Initial Oxidation of Fe–Al and Fe–Cr–Al Alloys: Cr as an Alumina Booster", Oxidation of Metals **76**, 331–346 (2011).

V **Nurmi, E.**, Wang, G., Kokko, K., Vitos, L., "Assessing the elastic properties and ductility of Fe–Cr–Al alloys from ab initio calculations", Philosophical Magazine **96**, 122–133 (2016).

VI **Nurmi, E.**, Tuuli, E., Levämäki, H., Kokko, K., Leiro, J., Vitos, L., "Directional Young's modulus of single-crystal and cold-rolled titanium from ab initio calculations: Preferred crystal orientation due to cold rolling", Philosophical Magazine **96**, 2736–2751 (2016).

Comment on my own contribution: In all publications I participated in the planning of the research, performing the computations, analysing the results, and writing the report. In the publications V and VI I was the main author.

Other publications (not included in the thesis):

I Delczeg-Czirjak, E. K., **Nurmi, E.**, Kokko, K., Vitos, L., "Effect of long-range order on elastic properties of $Pd_{0.5}Ag_{0.5}$ alloy from first principles", Phys. Rev. B **84**, 094205 (2011).

II Hoffmann, M., Marmodoro, A., **Nurmi, E.**, Kokko, K., Vitos, L., Ernst, A., Hergert, W., "Elastic anomalies and long/short-range ordering effects: A first-principles investigation of the $Ag_cPd_{1-c}$ solid solution", Phys. Rev. B **86**, 094106 (2012).

III Airiskallio, E., **Nurmi, E.**, Väyrynen, I., Kokko, K., Ropo, M., Punkkinen, M., Johansson, B., Vitos, L., "Magnetic origin of the chemical balance in alloyed Fe–Cr stainless steels: First-principles and Ising model study", Computational Materials Science **92**, 135–140 (2014).

# Contents

# 1 Introduction

Titanium and steel are commonly considered to be strong materials. There are a countless number of applications for those metals, including construction, car industry and aviation as well as household equipment. Steels are iron alloys containing also other metals and carbon while titanium is a pure chemical element. Carbon steel iron is also a useful material but tends to oxidise easily. By the addition of specific alloying elements the corrosion resistance can be improved.

Metallurgy is the old branch of science that deals with previous questions. In ancient times the ability to build metallic tools was a significant step forward in cultures. The scientific revolution and the increasing understanding of the microstructure of materials made it possible to adjust the properties of metal alloys in a more advanced way. Thus, a vast number of experimental research have been carried out about metal alloys and pure metals including iron alloys and titanium. The invention of quantum mechanics made it also possible to calculate the properties of alloys without experiments, at least in principle. The complexity of the calculations and the enormous number of atoms needed in simulations made it anyhow impossible to perform the calculation prior to the invention and the fast development of computers.

In the present work the corrosion resistance and ductility of iron-based alloys as well as the elasticity and ductility of titanium have been investigated using first principles calculations. Calculations are performed using Exact Muffin-tin orbitals method [1], based on the density functional theory [2, 3]. In addition to the original research papers the thesis consists of a brief explanation of the theoretical background of alloys, previous studies, calculation methods and results.

# 2 Background

## 2.1 Modern Alloy Theory

Solid state metals have typically ordered crystal structure. A piece of metal can be a single crystal but more often materials are polycrystalline. An alloy is formed when metals (or metal and other element) are mixed with varying composition. Mixed elements can either form separate phases or mix perfectly forming a solid solution. In the solid solution the atoms of different chemical elements form together a crystal structure. Typically the mechanism of solid solution is either interstitial or substitutional (Fig. 2.1). In the interstitial mechanism the solute atoms end up between the solvent atoms, while in the substitutional mechanism some atoms of the original crystal are replaced with the solute atoms. [4–6]

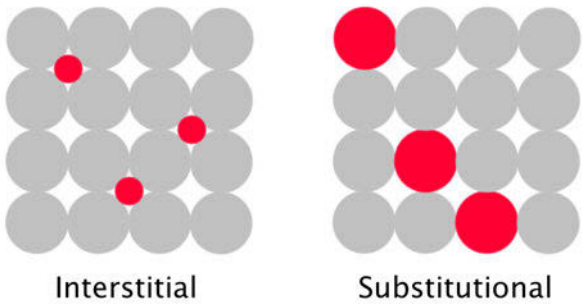


FIGURE 2.1: Schematic figure of interstitial and substitutional alloys. The gray color is representing the solvent atoms and the solute atoms are red.

In the present work the investigated alloys are considered to be substitutional and randomly distributed with the given average percentages of solute and solvent atoms. This type of alloys can be modelled using coherent potential approximation (described in section 3.5) in the calculations.

## 2.2 Crystal Symmetry

The enormous number of atoms in metal samples would be impossible to consider separately. However, the symmetry in crystalline solids can be utilized in modelling. In the concept of Bravais lattice the crystals are approximated to consist of infinite number of repeated unit cell structures. This is a reasonable assumption on the ground of the difference between the order of magnitude in atomic and crystals scale. The Bravais lattice represents crystals by set of translation vectors (primitive vectors) between equivalent lattice positions and the basis of atoms at the positions. The formation of iron lattice with unit cells is demonstrated in Figure 2.2. Altogether there are fourteen different Bravais lattices. [7, 8]

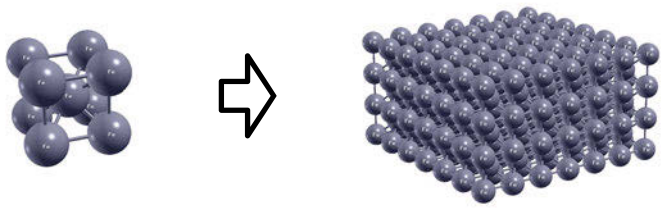

FIGURE 2.2: The unit cell of the body centered cubic structure of iron and a section of the crystal consisting of the unit cells [9]

Depending on the structure, the amount of symmetry varies. For example, in body centered cubic lattices (e.g. Figure 2.2) the structure remains equivalent in 90 degree rotations about three main symmetry axes. In addition to 90° rotation symmetry cubic structures are also symmetric in 120° rotations about the body diagonal axes and 180° rotations about the centers of opposite cube edges. Compared to this, there is much less symmetry in the

hexagonal close packed structure (Figure 2.3). There are only three 180° and one 120° rotation symmetry axes in the hexagonal lattice. [7, 8, 10, 11]

In the present work the considered lattices are body centered cubic (bcc) for iron alloys (Figure 2.2) and hexagonal lattices for titanium (Figure 2.3). Due to the lattice deformations in the calculations of elasticity orthorhombic and monoclinic structures are also needed.

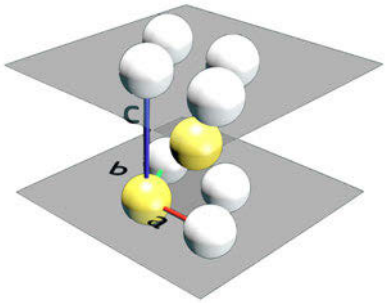


FIGURE 2.3: The hexagonal close package (hcp) unit cell

## 2.3 Mechanical Properties

The elastic properties of solid state materials are generally described using the framework of Hooke's law, which is based on the assumption that materials obey the linear relation between the stress and the strain, in general form:

$$\text{Elastic modulus} = \frac{\text{Stress}}{\text{Strain}}. \tag{2.1}$$

With small stress and strain values the theory describes well the elasticity for many solids. For isotropic materials the macroscopic elasticity is typically described using four elastic moduli: Young's modulus ($E$) that corresponds the tensile strain, the shear modulus ($G$), Bulk modulus ($B$) corresponding to the homogeneous (pressure kind of) stress around the specimen and Poisson's ratio ($\nu$) defined as the ratio of transverse strain to longitudinal strain. Every set of two of elastic moduli are mutually independent, which means

that when two of the moduli are known, there are formulas to solve the other two.

For engineering purposes, the macroscopic (and polycrystalline) elastic moduli ($B$,$G$,$E$ and $\nu$) are most useful way to describe the elasticity, whereas in the point of view of materials physics, the single crystal (often anisotropic) elastic constants $c_{ij}$ are more interesting. Single-crystal elastic constants are also applicable in the case of macroscopic single crystal structures. The symmetry of crystals typically reduces the number of independent elastic constants. For example, in bcc structure there is three independent constants and in hcp structure there is five. [1, 12]

The elastic constants $c_{ij}$ are usually defined by using Voigt notation, where the stress $\vec{\sigma}$ and the strain $\vec{\varepsilon}$ are symmetric linear mappings from three-dimensional real number space to three-dimensional real number space, $L : \mathbb{R}^3 \to \mathbb{R}^3$, written as six-component vectors
$\vec{\sigma} \equiv \begin{pmatrix} \sigma_1 & \sigma_2 & \sigma_3 & \sigma_4 & \sigma_5 & \sigma_6 \end{pmatrix}^T$ and $\vec{\varepsilon} \equiv \begin{pmatrix} \varepsilon_1 & \varepsilon_2 & \varepsilon_3 & \varepsilon_4 & \varepsilon_5 & \varepsilon_6 \end{pmatrix}^T$.
Indices of the mapping are contracted matrix notations, for the strain (for the stress correspondingly):

$$L_\varepsilon = \begin{pmatrix} \varepsilon_{11} & \frac{1}{2}\varepsilon_{12} & \frac{1}{2}\varepsilon_{13} \\ \frac{1}{2}\varepsilon_{12} & \varepsilon_{22} & \frac{1}{2}\varepsilon_{23} \\ \frac{1}{2}\varepsilon_{13} & \frac{1}{2}\varepsilon_{23} & \varepsilon_{33} \end{pmatrix} \equiv \begin{pmatrix} \varepsilon_1 & \frac{1}{2}\varepsilon_6 & \frac{1}{2}\varepsilon_5 \\ \frac{1}{2}\varepsilon_6 & \varepsilon_2 & \frac{1}{2}\varepsilon_4 \\ \frac{1}{2}\varepsilon_5 & \frac{1}{2}\varepsilon_4 & \varepsilon_3 \end{pmatrix} \tag{2.2}$$

.

Hooke's law can now be written as a matrix equation

$$\vec{\sigma} = (c_{ij})\vec{\varepsilon},$$

where $(c_{ij})$ is the $6 \times 6$ stiffness matrix consisting of the elastic constants. Depending on the symmetry, the number of independent elements varies, though the matrix is always symmetric. For example, in the cubic symmetry there are three independent coefficients and for the hexagonal symmetry five.

The elastic constants $c_{ij}$ carry the full information of the elasticity of the structure in all directions. Thus, the elastic moduli ($B$,$G$,$E$ and $\nu$) can be written using the $c_{ij}$-constants or compliance constants $s_{ij}$, that are matrix elements of the inverse matrix of the $(c_{ij})$. [12, 13]

## 2.4 Properties of Industrial Alloys

### 2.4.1 Surface Treatments

The surface properties of alloys can be improved by surface treatments. There are numerous surface treatment methods, consisting of chemical, mechanical and thermal treatments in addition to coating methods. Some typical properties to improve in materials are appearance, strength and the resistance against corrosion. The intended use of the alloy prescribes the necessary treatments. [14]

### 2.4.2 Stainless steels

The oxidation resistance of stainless steels is based on the formation of protective layers on the surface of metals due to oxidation. The protectiveness of the formed layers depends on the ratios of alloyed elements.

The complete mechanism behind the critical concentrations for corrosion resistance is not known, but investigations based on thermodynamics and diffusion have been performed. The type and level of protection of oxides depends on a variety of things. The major factor is of course which metal oxidises. For example, iron oxides are not typically very protective while aluminium oxides are, but also the thickness and texture of the oxide matters. In the high temperature oxidation of iron, multilayered oxide-scales are formed containing three types of oxides: FeO, $Fe_3O_4$ and $Fe_2O_3$. The chromium forms only one type of oxide: $Cr_2O_3$. This oxide forms a quite protective oxide layer. For Fe-Cr alloys the addition of aluminium boosts the formation of stable, protective, layer on the surface. This kind of alloys have been utilized commercially in many materials. [15]

Fe-Al is one of the best alloys regarding high temperature corrosion resistance, when the concentration of Al is at least 10-20 at.%. However, the addition of aluminium causes the weakening in the mechanical properties in the point of view of practical applications; High Al content makes the alloy brittle. Addition of third component to the alloy is often a solution on to the problem. This kind of alloys have also been investigated in the present work.

### 2.4.3 Rolling

In chapter 2.3 the elasticity of materials was introduced. In the framework of elasticity, the structure deformations are temporary, occurring only while there is stress. However, when the magnitude of stress is big enough, permanent structure deformations take place. This kind of deformations are called to be plastic. Plastic deformations of metals are useful in many ways. There are a lot of metal forming processes, one of which is rolling. In the rolling process a metal sheet is passed through a pair of rolls or several pairs of rolls. Rolling can typically be categorized either cold rolling or hot rolling. [16, 17]

Rolling processes at the temperature lower than half of the melting point of a metal can be considered to be cold rolling and the processes at higher temperature than that is termed hot rolling. On the other hand, the recrystallization temperature can be seen as the separating temperature between the processes. Altogether, there is no strict division between hot and cold rolling, and the rolling processes taking place around half of the melting point temperature are also known as warm rolling. When the working of metals is performed in temperatures higher than recrystallization temperature, it is easier to deform metal in useful shapes and there is less residual stress compared to cold working. On the other hand, cold working strengthens materials. In the present work, cold rolling is the investigated process. [16, 18]

In addition to strengthening also ordering is taking place in cold rolling of metals. For hcp-structures the types of textures forming during cold rolling depend on the c/a-ratio of a material compared to the ideal c/a-ratio. For example, the c/a-ratio for titanium is lower than ideal ($c/a < 1.633$). Due to cold rolling the materials having this kind of c/a-ratio form textures where the basal poles are tilted 20–40 degrees towards transverse direction (Figure 2.4). [19]

### 2.4.4 Alloying

Pure metals are useful only in very specific types of industrial applications, for example when high electrical or thermal conductivity is needed. Still, in the most cases metal alloys are used. One of the main reasons for alloying is the improvement of mechanical properties. Typically pure metals are weaker than alloys and properties like strength, heat resistance and weldability among other properties can be improved by alloying. [4, 6]

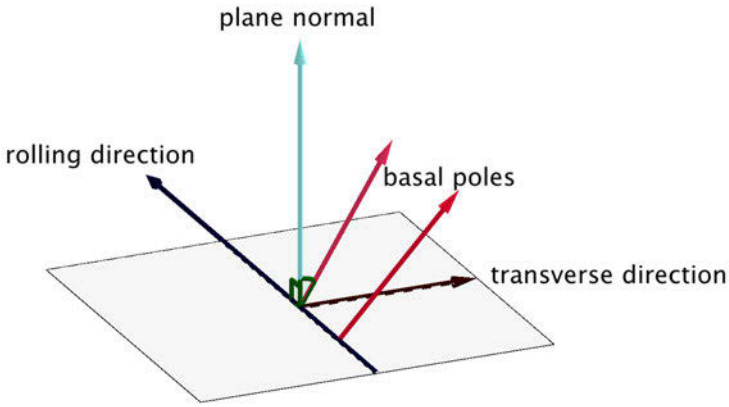


FIGURE 2.4: Schematic figure of the tilting of the basal poles of hcp crystals in cold rolling [20]

A small addition of carbon ($< 0.3$ wt.%) in iron cause moderate strength and excellent ductility for the alloy. This alloy is a very typical, cost efficient, commercial alloy known as low-carbon steel, used in i.e. bridges and ships. Also higher carbon additions are used when the steel is called correspondingly medium- and high-carbon steels. Addition of other alloying element e.g. nickel or chromium improve the corrosion resistance of the alloy and this kind of iron alloys are known as stainless steels (described in subsection 2.4.2). [21, 22] One challenging area of materials design is the air plane industry where the alloys have to be simultaneously light but also meet different mechanical requirements in harsh environments [23].

## 2.5 Experimental Studies

Traditionally materials research has been an experimental science, and thus the simulations of this thesis can mostly be verified also experimentally.

X-ray diffraction is a useful method for the analysis of the arrangement of atoms in crystal structure and also the grain orientation of the specimen. On the other hand, there are more suitable methods for the investigations of

chemical composition of materials, surface topography and oxides. Chemical states and chemical properties can be analysed with spectroscopic methods such as X-ray photoelectron spectroscopy (XPS) or Auger electron spectroscopy (AES). These techniques are also usable for depth profiling. Other methods used for surface investigations are based on microscopy or probe techniques, for example atomic force microscopy (AFM). [24, 25]

Elastic constants are measured typically by using acoustic waves. The elastic constants can be calculated by measuring the sound propagation on the material, being proportional to the square of the sound speed and the mass density of the sample. [26, 27]

## 2.6 Previous *Ab Initio* Studies

First principles studies for the surface concentrations of solute metals in alloys are previously presented e.g. in articles [28, 29]. The calculations were performed using full-potential Korringa-Kohn-Rostoker method (KKR) and Linear Muffin-tin Orbitals method (LMTO). In these investigations the tendency of surface segregation is presented for different impurity solute atoms in iron [28] and other transition metals [29]. The results suggest that, as single impurity atoms, vanadium and chromium antisegregate at the surface of iron. Segregation and antisegregation are the key phenomena also in the corrosion resistance investigations of the present work. A publication of our research group [30] explains the mechanism that drives the Cr to the surface of Fe-Cr alloy with Cr bulk concentration higher than $9 - 13$ at.% causing a significant improvement in the corrosion resistance.

In addition to the numerous experimental results for elastic constants, the topic is nowadays widely studied by using computational methods. The results for hcp-titanium elastic constants calculated using tight-binding (TB) method was presented in article [31]. Ductility-brittleness calculations, corresponding to the present work, have been among others published for Fe-Ni, Fe-Mn, Fe-Ga and Ni-Al-based alloys [32–34] .

## 2.7 Objectives of the Present Work

The investigated topics of this thesis are the surface chemistry of iron alloys, especially oxidation, and the mechanical properties of iron alloys and titanium.

The first objective of the research is to describe and build a model of the phenomena behind the corrosion resistance of iron alloys. The validity of the model is confirmed by reproducing the experimentally proven corrosion resistance results by *ab initio* calculations. The second objective is to produce new data concerning optimal alloying ratios for corrosion resistance.

The corresponding aims are set for the investigation of mechanical properties. Unit cell elasticity can be simulated by varying the form and the volume of the cell in calculations. The experimental reference values for pure metal elastic constants are typically easy to find. On the other hand, *ab initio* methods are capable to create a lot of alloy elasticity data without time consuming and expensive experiments. In addition to elastic properties also the modelling of the ductility of metals is an important objective of the present work.

# 3 Methods

## 3.1 Density Functional Theory

Quantum mechanics describe atomic scale phenomena in the most exact way. It is quite straightforward to form the equations for the interactions between nuclei and electrons in crystal structures. Much more challenging task is to solve the equations. Thus, in every numerical calculation of the present work, the most fundamental and most complex task before any other investigations is to approximate a solution for the static Schrödinger equation for the electrons of the system:

$$[\frac{-\hbar^2}{2m_e}\sum_{i=1}^{N}\nabla_i^2 + \sum_{i=1}^{N}V(\mathbf{r}_i) + \sum_{i=1}^{N}\sum_{j<i}U(\mathbf{r}_i,\mathbf{r}_j)]\Psi = \epsilon\Psi. \tag{3.1}$$

In the equation $m_e$ is the electron mass, $N$ the number of electron in the system and $\mathbf{r},\ldots,\mathbf{r_N}$ are the spatial coordinates of the electrons. $V(\mathbf{r}_i)$ is the atom nuclei induced potential energy of an electron, and electron-electron interactions are presented with potential functions $U(\mathbf{r}_i,\mathbf{r}_j)$. The electron wave function $\Psi$ depends on all of the electron coordinates: $\Psi = \Psi(\mathbf{r},\ldots,\mathbf{r_N})$ and the minimum of $\epsilon$ is the ground state energy of the system. For simplicity, electron spin is neglected in the equation. This equation needs to be solved for all the considered atomic setups. [35, 36]

Although the exact equation (3.1) for the ground state of electrons can be formed, it cannot be solved analytically. The problem is that all the electrons interact with each other. As a matter of fact, even for an equation of three interacting objects, there is no closed-form solution. Thus, estimations and numerical methods are needed. An approximated solution to this problem can be found by treating the electrons as electron gas with a density of $\rho(\mathbf{r})$. This is the fundamental set up in the density functional theory (DFT). The

key idea in DFT is to minimize the total energy functional $E[\rho]$ of the system, where $\rho = \rho(\mathbf{r})$ is the electron density. The Hohenberg-Kohn theorems state that all the ground state properties of the N particle system could be, in principle, solved from the total energy functional [2, 35, 36]:

**Theorem 3.1** (existence theorem)**.** *Let $\rho(\mathbf{r})$ be the single-particle density of a non-degenerate ground state of an interacting electron system in an external potential $V_{ext}$, and let $\rho'(\mathbf{r})$ correspond in the same manner to $V'_{ext}$. Then $\rho(\mathbf{r}) = \rho'(\mathbf{r})$ implies $V_{ext} = V'_{ext} + C$, where $C$ is a constant.*

**Theorem 3.2** (variation principle)**.** *The total energy of the N-particle system $E[\rho]$ is minimized by the ground-state electron density, if the trial densities $\rho(\mathbf{r})$ are restricted by the conditions $\rho(\mathbf{r}) \geq 0$ and $N[\rho] \equiv \int \rho(\mathbf{r}) d^3\mathbf{r} = N$.*

## 3.2 Kohn-Sham Equations

Hohenberg-Kohn theorems are essential for DFT, but from the point of view of the practical calculations these purely theoretical and descriptive results give little help. Calculation methods are needed in addition of the theorems. Kohn-Sham Equations (3.2, 3.3 and 3.4) provide a solution to the problem:

$$V_{eff}(\mathbf{r}) := V_{ext}(\mathbf{r}) + \int \frac{2\rho(\mathbf{r}')}{|\mathbf{r} - \mathbf{r}'|} d^3\mathbf{r}' + \frac{\delta E_{xc}[\rho]}{\delta \rho(\mathbf{r})}, \tag{3.2}$$

$$[\frac{-\hbar^2}{2m_e}\nabla^2 + V_{eff}(\mathbf{r})]\Psi_i(\mathbf{r}) = \epsilon_i \Psi_i(\mathbf{r}) \tag{3.3}$$

$$\rho(\mathbf{r}) = \sum_{i \in O} |\Psi_i(\mathbf{r})|^2. \tag{3.4}$$

The first equation (3.2) is the formula to calculate the effective potential $V_{eff}(\mathbf{r})$ in terms of an external potential function $V_{ext}(\mathbf{r})$, electron density $\rho(\mathbf{r})$ and the functional derivative of the exchange-correlation energy $E_{xc}[\rho]$. The external potential is caused by the nuclei of the atoms while the exchange-correlation energy (explained in more detail in the section 3.3) includes all the non-classical and many-particle interactions. The second equation (3.3) corresponds the Schrödinger equation for the effective potential for

non-interacting electrons and the third equation (3.4) is the formula for calculating the electron density using the solution of the effective Schrödinger equation (3.3). [3]

Kohn-Sham equations can be applied as the basis of algorithm for numerical calculations: The iteration is started using some initial value for the electron density $\rho(\mathbf{r})$ or effective potential $V_{eff}(\mathbf{r})$. The equation (3.3) is solved using the effective potential. In the first iteration the non-interacting electron system is solved, in the further iterations the interactions are included in the effective potential. By using the solved wave function $\Psi_i(\mathbf{r})$, the new electron density $\rho(\mathbf{r})$ (3.4) can be calculated by summing over the occupied states $O$ and again the new effective potential (3.2) can be calculated. [36]

## 3.3 Exchange and Correlation in Electron Systems

All the terms of the equation (3.2) can be explicitly calculated for a given electron density except the exchange-correlation energy $E_{xc}[\rho]$. This is the part of the equation that have to be approximated in the self-consistent calculations of the Kohn-Sham Equations (3.2–3.4). In the local density approximation (LDA) and local spin density approximation (LSD) the electron density is approximated with uniform electron gas, depending just on the electron density at each point. Local density approximations are simplest estimations for exchange and correlation but give generally fairly good results. In addition to this, efforts to improve the approximation have often resulted less accurate results. [37–41]

Although many attempts to improve LDA have been unsuccessful, there is also a lot of successful more advanced exchange-correlation models. In the general gradient approximations (GGA), in addition to the electron density, also the gradient of the density is taken in to account. The kinetic energy density or the Laplacian of the electron density is taken into account in the meta-GGA. In the hybrid functional approach the local exchange energy is partly replaced with the exact exchange energy density. [41–43] Perdew et al. [44] describe the exchange-correlation functionals with the metaphor of Jacob's ladder. The first rung of the ladder is the local spin density approximation, second GGA and in this way the ladder is climbed until the exact

results are reached. However,the next rung in the ladder does not automatically improve the accuracy for every system but decreases to probability to fail. [44–46]

## 3.4 Exact Muffin-Tin Orbitals Method

In the exact muffi-tin orbitals method (EMTO) the Kohn-Sham equations are solved by assuming the potential functions to have muffin-tin like form (Figure 3.1), where the potential consists of spherically symmetric parts around the nuclei of the atoms. One sphere consists of the inner 'hard sphere' part having radius $a$ and outer 'potential sphere' with radius $s$. The $a$-spheres should not intersect whereas the $s$-spheres overlap each other. Outside the spheres the potential is defined to have a constant value $V_0$. Thus, the potential function has the form:

$$V(\mathbf{r}) = V_0 + \sum_R [V_R(\mathbf{r}_R) - V_0], \tag{3.5}$$

where $\mathbf{r}_R = \mathbf{r} - \mathbf{R}$ and $V_R(r_R) = V_0$, when $r_R > s_R$. $\mathbf{R}$ is the position vector of the nucleus of the considered atom. The potential function $V_R(r_R)$ is the radius ($r$) dependent part, consisting of the $a$- and the $s$-sphere.

The exact muffin-tin orbitals are constructed using different basis functions inside the potential spheres and in the interstitial region. The orbitals are constructed in the interstitial region using screened spherical waves and they behave as spherical harmonic inside their own hard sphere but disappear inside other hard spheres. The orbitals inside potential spheres consist of partial waves that are solutions for the radial Schrödinger equation multiplied with spherical harmonics. In order to join the solutions smoothly, also free-electron solutions are needed. The exact muffin-tin orbitals $\Psi_i(\mathbf{r}_r)$ are presented as a weighted sum of the different basis function parts. The coefficients of the sum are solved by using the conditions concerning the smoothness of the solution. This problem reduces to the solving of the kink cancellation equation for every $R'$ [1, 47]:

$$\sum_{RL} a_{R'} [S^a_{R'L'RL}(\kappa^2) - \delta_{R'R}\delta_{L'L} D^a_{Rl}(\epsilon)] v^a_{RL,i} = 0, \tag{3.6}$$

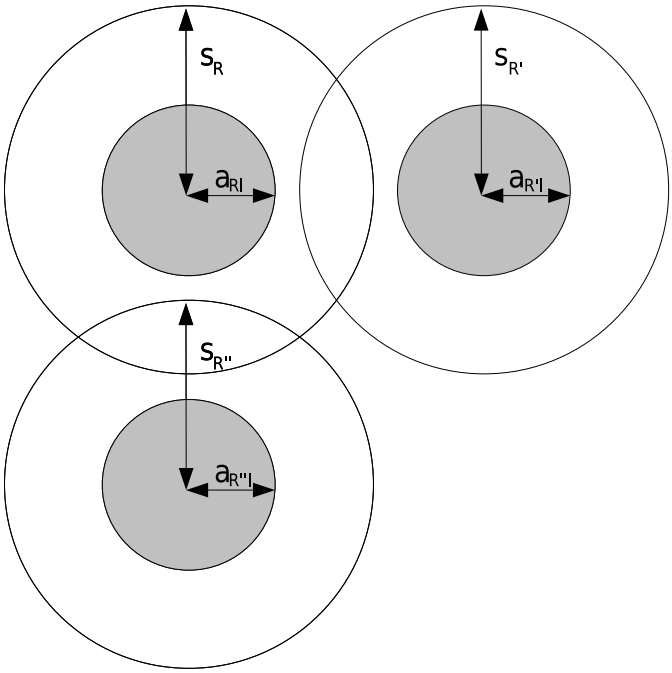


FIGURE 3.1: Division of space in the Exact Muffin-Tin Orbitals method. The radii $a$ and $s$ are indexed by the position vectors of atomic nuclei $\mathbf{R}$ and the angular quantum number $l$.

where $a_{R'}$ is the hard sphere radius, $S^a_{R'L'RL}(\kappa^2)$ the slope matrix with energy values $\kappa^2$, $D^a_{Rl}$ the logarithmic derivative of the screened spherical wave indexed by the hard sphere radius $a$, the atomic position $R$ and the quantum number $l$. The $v^a_{RL,i}$ are expansion coefficients, determined from the condition that the expansion should be a solution of the equation (3.3) in the entire space.

### 3.4.1 Full Charge Density Technique

There are different ways to consider the interstitial region between spherical atomic potentials in the muffin-tin methods. The atomic sphere approximation neglects the interstitial "muffin-pan" region by assuming there to be zero

kinetic energy[48, 49]. For simple metals the accuracy is decent, but for complex calculations more advanced methods are needed [50].

More accurate results can be achieved by using the full-potential formalism, where the potential of the interstitial region is optimized [50–52]. Similar accuracy but higher efficiency can be achieved by using full charge density technique (FCD). In the FCD technique the full charge density is calculated. After that the total energy of the system is calculated by using the charge density. EMTO method gives exact solutions for single-electron states corresponding the potential used. Because of this EMTO is ideal for FCD calculations. [1, 47, 53, 54]

### 3.4.2 Accuracy in Alloy Calculations

Due to the exact form of the EMTO orbitals in the interstitial region of atoms high accuracy can be gained also in alloy calculations. However, the right numerical parameters are needed for the convergence of the self-consistent energy calculations. [1]

## 3.5 Coherent Potential Approximation

There are two major methods to perform multi component metal alloys calculations. The first is the supercell approach, where the random alloying of the atoms is modelled by using cells with high number of atoms and some quasirandom configuration of the atoms. The downsides of this method are the problematic nature of randomness and the huge number of the atoms needed to simulate systems realistically.

The other approach to alloy calculations is the so called coherent potential approximation (CPA), which is based on the assumption, that the alloy may be replaced by an ordered effective medium, the parameters of which are determined self-consistently. In the CPA method the Kohn-Sham equations (3.2 – 3.4) are first solved separately for each of the alloying components. For the next step the surroundings around the considered atom are averaged using the separate alloy components solution weighted by the concentration of the components. The Kohn-Sham equations are solved again for all the alloying components using this new effective surrounding. This iteration is continued until the convergence is reached. The CPA method gives often

very realistic results, though the convergence is a problematic issue for some materials and alloy components concentration ratios. [1, 36]

The coherent potential approximation cannot take into account the charge transfer effects or statistical fluctuations of the chemical composition of an alloy. This is due to the single-site approximation used in CPA [36]. This limitation does have slight effect in the accuracy of calculations, depending on the investigated system. On the other hand, CPA makes it possible to perform alloy calculations without huge super-cell structures. In addition to these two approaches, there is also a CPA method that goes beyond the single-site approximation. KKR Nonlocal CPA is based on cluster generalization of KKR-CPA-method [55], which makes it possible to investigate short-range ordered systems using CPA-technique [56].

## 3.6 Elastic Constants and Elastic Moduli

The well-defined result of CPA methods is typically the total energy of the given crystal structure. Thus, elasticity of materials can be simulated by expressing the total energy in terms of the lattice strain. It can be shown that the total energy change upon strain can be written as a Taylor expansion:

$$E(\varepsilon_1, \varepsilon_2, \ldots, \varepsilon_6) = E(0) + \frac{1}{2} V \sum_{i,j=1}^{6} c_{ij} \varepsilon_i \varepsilon_j + \mathcal{O}(\varepsilon^3), \tag{3.7}$$

where $\varepsilon_1, \varepsilon_2, \ldots, \varepsilon_6$ are the strain matrix component (2.2) according to the Voigt notation. $E(0)$ is the energy for unstrained lattice, $V$ the volume of the cell and $c_{ij}$ the elastic constants. [1]

By using these results, the elastic coefficients $c_{ij}$ can be solved by performing a set of deformations and calculating the total energy of the structure. For example, for a monoclinic volume conserving deformation the matrix (2.2) has the form:

$$L_\epsilon + I = \begin{pmatrix} 1 & \delta & 0 \\ \delta & 1 & 0 \\ 0 & 0 & \frac{1}{1-\delta^2} \end{pmatrix},$$

where $\delta$ is the distortion. The corresponding energy change according to (3.7) is now

$$\Delta E = 2 c_{44} V \delta^2 + \mathcal{O}(\delta^4). \tag{3.8}$$

Typically total energies are calculated for values $\delta = 0.00, 0, 01, \ldots, 0.05$.

Elastic constant $c_{44}$ can now be solved, by fitting equation (3.8) to the distortions and calculated energies. Other elastic constants can be solved with different deformations correspondingly. The number of deformations needed depends on the number of independent elastic coefficients to be calculated. [1]

# 4 Results

## 4.1 Iron Alloys

### 4.1.1 Surface Chemistry

The oxidation reaction of a metal ($M$) has the general form

$$a\mathrm{M} + \frac{b}{2}\mathrm{O}_2 \rightarrow \mathrm{M}_a\mathrm{O}_b.$$

Despite the fact, that the equation is quite simple, a lot of complex dynamics are involved in the processes. In order to continue the reaction, one or both reactants must diffuse to a proper interface for the reaction. Formation of protective oxide scales on the metal surfaces prevents this movement and thus makes the material corrosion resistant. In this work, the high temperature is considered to mean roughly temperatures over 1000 K. The investigated corrosion is here limited to the oxidation due to pure oxygen.

The corrosion resistance of iron can be improved by adding an alloying component that causes formation of protective oxide layers on the surface of the alloy. The surface chemistry and thermodynamics behind the formation of protective scales was analysed in papers I – IV. The considered corrosion resistant binary alloys in the present work are Fe-Al and Fe-Cr.

Fe-Al is one of the best corrosion resistant alloys at high temperatures. In order to be corrosion resistant the Al concentration in the alloy should, however, be at least $10 - 20$ at.%. Unfortunately, this amount of Al makes the alloy brittle. This problem can be solved by adding e.g. chromium to the alloy, which makes it possible to get the same properties with lower Al concentration. Corresponding results are presented in paper I, where the addition of vanadium is suggested to shift the corrosion resistance properties of Fe-Cr alloy towards lower Cr concentrations. This phenomenon represents

the so called third element effect (TEE). In the third element effect the properties of a binary alloy is changed by addition of third component that does not have a direct role in corrosion resistance but participates in a more complex way in this phenomenon.

In the paper I the addition of vanadium turned out to lower the bulk chemical potential difference curve $(\mu_{Fe} - \mu_{Cr})^{\text{bulk}}$ at small Cr concentrations which suggests vanadium to have a positive effect to the corrosion resistance of Fe-Cr alloy. The added vanadium occupies virtually solely the bulk sites. However, the predicted effects on the surface properties are significant.

Also for Fe-Cr-Al alloys bulk effects are significantly related to the surface properties and thus to corrosion resistance too. The Al depletion at the surface zone is considered to be one of the main causes for the breakdown of the oxidation resistance [57]. According to the results of paper II, the key factor in the corrosion resistance mechanism in the third element effect for Fe-Cr-Al is the coexistent Cr depletion that helps to maintain a sufficient Al content in the depleted zone. Experimental results for this system was presented and analysed using first principles total energy data in paper IV. The boosting effect of Cr on the growth of the protective alumina scale on Fe13Al and Fe10Cr10Al alloys have been investigated using X-ray photoelectron spectroscopy (XPS). The results show a clear surface-bulk Fe-Al concentration exchange as effect of Cr. 10 at.% addition of Cr shifts the Fe-Al surface balance by increasing Al concentration by 30%. In this way Cr improves the high temperature oxidation resistance. At 700 °C both Fe and Al show significant bulk-surface diffusion whereas Cr diffusion is negligible. At this temperature only Al is oxidized. At room temperature there is no cationic diffusion.

Also the study of paper III supports the result that the oxidation resistance boosting effect of Cr is significantly related to the bulk effects. The chemical potential differences $\mu_{Fe} - \mu_{Cr}$ and $\mu_{Fe} - \mu_{Al}$ have been calculated in bulk and surface in at.% range of 0 to 20 for chromium and 0 to 25 for aluminium. Experimental investigations have been performed using Auger electron spectroscopy (AES), atomic force microscope (AFM) and optical microscope for four specimen, prepared by induction melting under argon: Fe-13Al, Fe-18Al, Fe-23Al and Fe-10Cr-10Al.

Experimental results show that Fe-13Al does not form the protective oxide scale but other compounds do, and the protective layers are mainly consisting of Al-oxides. Increasing of the Al content for Fe-Al from 13 to 18 at.% makes the alloy resistant to oxidation at 1000 °C. Based on the atomic

fraction results of the experiments, four zones of oxidation can be defined in the specimen: Surface zone, Saturation zone, Inversion zone and deflection zone. It can be seen that, Al driving force to surface is mainly due to the bulk properties and is not very sensitive to the type of surface. Also the self-healing properties are to a large extend determined by the bulk part of the alloy. Increasing of the Cr concentration in bulk has two effects: The Al-content at the surface increases and Cr is also found at the surface. Computational results show that for the $\mu_{Fe} - \mu_{Cr}$ the bulk and surface curves intersect, whereas for $\mu_{Fe} - \mu_{Al}$ the surface curves are far above the bulk curves. Comparing of the experimental and computational results show a clear correlation between the composition of the oxide and the energetic balance $(\mu_{Fe} - \mu_{Cr})^{\text{bulk}} - (\mu_{Fe} - \mu_{Cr})^{\text{surf}}$.

### 4.1.2 Mechanical Properties

As noted above, high amounts of aluminium make Fe-Al alloy brittle. The corrosion resistance properties of Fe-Al and Fe-Cr-Al was discussed in previous section. The concentration limits for brittleness was investigated in paper V. The elastic constants for Fe-Cr-Al alloys were calculated in 0 – 20 at.% range for Cr and Al. The brittle/ductile-limit was estimated by using bulk modulus/shear modulus ratio and Cauchy pressure (elastic constant difference $c_{12} - c_{44}$). Using these estimations it can be seen that more than 5 – 10 at.% of aluminium makes the alloy brittle, depending on the amount of alloyed chromium.

### 4.1.3 Magnetism

Because of the ferromagnetism of iron, the considered iron alloys were modelled as magnetic alloys in the calculations. The previously reported magnetic transition [58] have been taken in to account in the calculation of the equilibrium volumes by choosing the fitted volumes far enough from the magnetic volume transition. For the further research of Fe-Cr-Al alloys the local magnetic moments for iron and chromium components were presented in paper V for different concentrations.

### 4.1.4 Surface Segregation

The spatially inhomogeneous nature of the surface of materials cause the segregation of different alloy components at the alloy surfaces [59]. From the computational point of view, the surface segregation can be modelled by separating the system into surface and bulk systems and performing comparisons for the thermodynamic potentials in the interchanges of atoms between the subsystems [60, 61]. This type of investigations was performed in papers I-IV, where the Fe-Cr-V and Fe-Cr-Al corrosion resistance properties are described with surface segregation related effects.

## 4.2 HCP Titanium

### 4.2.1 Mechanical Properties

Titanium is a strong corrosion-resistant material with low mass density, which makes it ideal for various purposes, including aviation and medical applications. At the first state of investigation the elasticity of titanium has been calculated for the single crystal structure. Due to the hexagonal symmetry of titanium, the calculation of its elastic constants is much more complicated than for the bcc structure of iron alloys.

In contrast to bcc structure, lattice relaxations are crucial to take into account when calculating the elasticity of hcp structures. The optimal c/a-ratio depends on the performed deformation of the structure. In addition to this, the position of the second hcp basis atom has to be relaxed. The total energetic effect of this relaxation is minor, but the unrelaxed atom caused error in the elastic constants of the same order of magnitude as the results in the research for paper VI.

### 4.2.2 Cold Rolling

Cold rolling makes polycrystalline titanium structurally oriented, basal poles tilted towards transverse direction as mentioned in the section 2.4.3. It is difficult to directly model the cold rolled structure computationally due to the big and varying size [62] of the grains. Nevertheless, the structure can be simulated by using trigonometric formulas and bulk results for hcp titanium. The obtained single crystal results can be converted to describe the properties

of cold rolled titanium. Young's modulus depending on the grain tilt angles and measurement angle in the rolling plane was presented in Paper VI. Also an estimation for the preferred tilt angle was presented.

# 5 Conclusions

In this thesis the oxidation of Fe-Cr, Fe-Al, Fe-Cr-V and Fe-Cr-Al alloys as well as the elasticity of Fe-Cr-Al alloys and titanium have been investigated. The main method in all the research have been full charge density exact muffin-tin orbitals method (EMTO) based on density functional theory (DFT). This *ab initio* method is used for calculating total energies for given periodic crystals. There is no possibility to directly simulate oxides or alloy dynamics using EMTO. However, in oxide environments the metal at the surface of an alloy tends to oxidise. Thus, by comparison of the chemical potential differences the preferred surface composition can be found and consequently also the oxides formed. Corrosion resistance is based on the formation of protective oxide scales, e. g. $Al_2O_3$. The formation of protective scales in a binary alloy can also be improved by so called third element effect (TEE), where a third alloying element in the bulk drives the metal for the protective oxide to the surface.

Elasticity can be calculated by simulating deformations. When the distortions to the structure are known and the corresponding total energies are calculated, the single crystal elastic constants can be solved. In calculation of the elasticity of Fe-Cr-Al there is not only question about mechanical properties of the material but also the optimization of the mixing ratios for corrosion resistant alloy. High amounts of aluminium make the alloy brittle, which can be avoided by adding third alloying element Cr. Brittleness calculations, based on the elastic constants, give the answer to the question how much there have to be these components in the alloy to get simultaneously corrosion resistant and ductile Fe-Cr-Al alloys.

For both corrosion resistance and elasticity investigations the first objective was to describe the phenomena and build a model of them. The second objective was to produce new data by using the models. Preferred surface compositions for Fe-Cr, Fe-Cr-V and Fe-Cr-Al were calculated and presented, and the results were within a good agreement with the previously published

and our own experimental results. Likewise the brittle/ductile model for Fe-Cr-Al described fairly well the phenomenon. For titanium single crystal results and angle dependent elastic moduli was presented. The models and graphs in the papers include also new data points that have not been published before.

# Bibliography


[1] Vitos, L., *Computational Quantum Mechanics for Materials Engineers* (Springer, London, 2007), pp. 16–22, 219–220 (See pp. 13, 18, 28, 30–32).

[2] Hohenberg, P., Kohn, W., "Inhomogeneous Electron Gas", Physical Review **136**, B864–B871 (1964) (See pp. 13, 26).

[3] Kohn, W., Sham, L., "Self-Consistent Equations Including Exchange and Correlation Effects", Physical Review **140**, A1133–A1138 (1965) (See pp. 13, 27).

[4] F, C., *Elements of Metallurgy and Engineering Alloys* (ASM International, 2008) (See pp. 15, 20).

[5] Reardon, A., *Metallurgy for the Non-Metallurgist, Second Edition* (ASM International, 2011) (See p. 15).

[6] Davis, J., *Alloying: Understanding the Basics* (A S M International, 2001) (See pp. 15, 20).

[7] Marder, M., *Condensed Matter Physics* (Wiley, Hoboken, 2010) (See pp. 16, 17).

[8] Kittel, C., *Introduction to Solid State Physics*, Fourth (Wiley, New York, 1971), pp. 4–25 (See pp. 16, 17).

[9] Kokalj, A., "Computer graphics and graphical user interfaces as tools in simulations of matter at the atomic scale", Computational Materials Science **28**, 155–168 (2003) (See p. 16).

[10] McKie, D., McKie, C., *Crystalline Solids* (Nelson, London, 1974) (See p. 17).

[11] "Space Groups in Real Space", in *Group Theory* (Springer Berlin Heidelberg, Berlin, Heidelberg, 2008), pp. 183–208 (See p. 17).

[12] Grimvall, G., *Thermophysical properties of materials* (North-Holland, 1986) (See p. 18).

[13] Voigt, W., *Lehrbuch der Kristallphysik* (Johnson Repr, New York, 1966) (See p. 18).

[14] Tunturi, P. J., *Korroosiokäsikirja* (Suomen korroosioyhdistys, Hanko, 1988) (See p. 19).

[15] Wolff, I., Iorio, L., Rumpf, T., Scheers, P., Potgieter, J., "Oxidation and corrosion behaviour of Fe-Cr and Fe-Cr-Al alloys with minor alloying additions", Materials Science and Engineering: A **241**, 264–276 (1998) (See p. 19).

[16] Askeland, D., *The science and engineering of materials* (Cengage Learning, Mason, Ohio, 2008) (See p. 20).

[17] McQuillan, A. D., McQuillan, M. K., *Titanium / by A.D. McQuillan and M.K. McQuillan*, English (Butterworths Scientific London, 1956), xix, 466 p., 1 leaf of plates : (See p. 20).

[18] Lenard, J. G., "1 - Introduction", in *Primer on Flat Rolling (Second Edition)*, edited by J. G. Lenard, Second Edition (Elsevier, Oxford, 2014), pp. 1–15 (See p. 20).

[19] Kocks, U. F., *Texture and Anisotropy : Preferred Orientations in Polycrystals and Their Effect on Materials Properties* (Cambridge University Press, Cambridge, 1998) (See p. 20).

[20] Hohenwarter, M., Borcherds, M., Ancsin, G., Bencze, B., Blossier, M., Éliás, J., Frank, K., Gál, L., Hofstätter, A., Jordan, F., Konečný, Z., Kovács, Z., Lettner, E., Lizelfelner, S., Parisse, B., Solyom-Gecse, C., Stadlbauer, C., Tomaschko, M., *GeoGebra 5*, `http://www.geogebra.org`, (Jan. 2018) (See p. 21).

[21] Smallman, R., Ngan, A., "Chapter 14 - Selected Alloys", in *Modern Physical Metallurgy (Eighth Edition)*, edited by R. Smallman and A. Ngan, Eighth Edition (Butterworth-Heinemann, Oxford, 2014), pp. 529–569 (See p. 21).

[22] Hosford, W. F., *Elementary Materials Science* (ASM International, 2012) (See p. 21).

[23] Sankaran, K. K., Mishra, R. S., "Chapter 1 - Introduction", in *Metallurgy and Design of Alloys with Hierarchical Microstructures*, edited by K. K. Sankaran and R. S. Mishra (Elsevier, 2017), pp. 1–20 (See p. 21).

[24] *Practical Materials Characterization* (Springer, New York, 2014) (See p. 22).

[25] Dahman, Y., "Chapter 2 - Generic Methodologies for Characterization*", in *Nanotechnology and Functional Materials for Engineers*, edited by Y. Dahman, Micro and Nano Technologies (Elsevier, 2017), pp. 19–45 (See p. 22).

[26] Lüthi, B., *Physical Acoustics in the Solid State* (Springer, 2017) (See p. 22).

[27] Leamy, H., Gibson, E., Kayser, F., "The elastic stiffness coefficients of iron-aluminum alloys – I experimental results and thermodynamic analysis", Acta Metallurgica **15**, 1827–1838 (1967) (See p. 22).

[28] Nonas, B., Wildberger, K., Zeller, R., Dederichs, P. H., "Energetics of $3d$ Impurities on the (001) Surface of Iron", Phys. Rev. Lett. **80**, 4574–4577 (1998) (See p. 22).

[29] Ruban, A. V., Skriver, H. L., Nørskov, J. K., "Surface segregation energies in transition-metal alloys", Phys. Rev. B **59**, 15990–16000 (1999) (See p. 22).

[30] Ropo, M., Kokko, K., Punkkinen, M. P. J., Hogmark, S., Kollár, J., Johansson, B., Vitos, L., "Theoretical evidence of the compositional threshold behavior of FeCr surfaces", Phys. Rev. B **76**, 220401 (2007) (See p. 22).

[31] Mehl, M. J., Papaconstantopoulos, D. A., "Applications of a tight-binding total-energy method for transition and noble metals: Elastic constants, vacancies, and surfaces of monatomic metals", Phys. Rev. B **54**, 4519–4530 (1996) (See p. 22).

[32] Ponomareva, A. V., Isaev, E. I., Vekilov, Y. K., Abrikosov, I. A., "Site preference and effect of alloying on elastic properties of ternary $B$ 2 NiAl-based alloys", Phys. Rev. B **85**, 144117 (2012) (See p. 22).

[33] Wang, H., Zhang, Z., Wu, R., Sun, L., "Large-scale first-principles determination of anisotropic mechanical properties of magnetostrictive Fe-Ga alloys", Acta Materialia **61**, 2919–2925 (2013) (See p. 22).

[34] Wang, G., Schönecker, S., Hertzman, S., Hu, Q.-M., Johansson, B., Kwon, S. K., Vitos, L., "Ab initio prediction of the mechanical properties of alloys: The case of Ni/Mn-doped ferromagnetic Fe", Phys. Rev. B **91**, 224203 (2015) (See p. 22).

[35] Sholl, D., Steckel, J. A., Sholl, *Density Functional Theory : A Practical Introduction* (Wiley, Hoboken, UNITED STATES, 2009) (See pp. 25, 26).

[36] Turek, I., Drchal, V., Kudrnovsky, J., Sob, M., Weinberger, P., *Electronic structure pd disordered alloys, surfaces and interfaces* (Kluwer academic publisher, 1997) (See pp. 25–27, 31).

[37] Tsuneda, T., *Density functional theory in quantum chemistry* (Springer, Tokyo, 2014) (See p. 27).

[38] Sholl, D., Steckel, J., *Density Functional Theory: A Practical Introduction* (Wiley, 2009) (See p. 27).

[39] He, L., Liu, F., Hautier, G., Oliveira, M. J. T., Marques, M. A. L., Vila, F. D., Rehr, J. J., Rignanese, G.-M., Zhou, A., "Accuracy of generalized gradient approximation functionals for density-functional perturbation theory calculations", Phys. Rev. B **89**, 064305 (2014) (See p. 27).

[40] Seminario, J. M., "An introduction to density functional theory in chemistry", in *Modern Density Functional Theory A Tool for Chemistry*, Vol. 2, edited by J. Seminario and P. Politzer, Theoretical and Computational Chemistry (Elsevier, 1995), pp. 1–27 (See p. 27).

[41] Burke, K., Perdew, J. P., Levy, M., "Semilocal density functionals for exchange and correlation: Theory and applications", in *Modern Density Functional TheoryA Tool for Chemistry*, Vol. 2, edited by J. Seminario and P. Politzer, Theoretical and Computational Chemistry (Elsevier, 1995), pp. 29–74 (See p. 27).

[42] Perdew, J. P., Burke, K., Ernzerhof, M., "Generalized Gradient Approximation Made Simple", Phys. Rev. Lett. **77**, 3865–3868 (1996) (See p. 27).

[43] Jones, R. O., "Introduction to Density Functional Theory and Exchange-Correlation Energy Functionals", in Computational Nanoscience: Do It Yourself! - Lecture Notes, Vol. 31, edited by J. Grotendorst, S. Blügel, and D. Marx, NIC Series (2006), pp. 45–70 (See p. 27).

[44] Perdew, J. P., Ruzsinszky, A., Tao, J., Staroverov, V. N., Scuseria, G. E., Csonka, G. I., "Prescription for the design and selection of density functional approximations: More constraint satisfaction with fewer fits", The Journal of Chemical Physics **123**, 062201 (2005) (See pp. 27, 28).

[45] Bretonnet, J.-L., "Basics of the density functional theory", AIMS Materials Science **4**, 1372 (2017) (See p. 28).

[46] Zhang, Y., Xu, X., Goddard, W. A., "Doubly hybrid density functional for accurate descriptions of nonbond interactions, thermochemistry, and thermochemical kinetics", Proceedings of the National Academy of Sciences **106**, 4963–4968 (2009) (See p. 28).

[47] Vitos, L., "Total-energy method based on the exact muffin-tin orbitals theory", Phys. Rev. B **64**, 014107 (2001) (See pp. 28, 30).

[48] Skriver, H. L., "The Atomic-Sphere Approximation (ASA)", in *The LMTO Method: Muffin-Tin Orbitals and Electronic Structure* (Springer Berlin Heidelberg, Berlin, Heidelberg, 1984), pp. 82–99 (See p. 30).

[49] Andersen, O. K., "Linear methods in band theory", Phys. Rev. B **12**, 3060–3083 (1975) (See p. 30).

[50] Ohno, K., Esfarjani, K., Kawazoe, Y., *Computational materials science: from ab initio to Monte Carlo methods*, Springer Series in Solid-State Sciences (Springer, Berlin, 1999) (See p. 30).

[51] Jansen, H. J. F., Freeman, A. J., "Total-energy full-potential linearized augmented-plane-wave method for bulk solids: Electronic and structural properties of tungsten", Phys. Rev. B **30**, 561–569 (1984) (See p. 30).

[52] Price, D. L., Cooper, B. R., "Total energies and bonding for crystallographic structures in titanium-carbon and tungsten-carbon systems", Phys. Rev. B **39**, 4945–4957 (1989) (See p. 30).

[53] Vitos, L., Kollár, J., Skriver, H. L., "Full charge-density calculation of the surface energy of metals", Phys. Rev. B **49**, 16694–16701 (1994) (See p. 30).

[54] Vitos, L., Abrikosov, I. A., Johansson, B., "Anisotropic Lattice Distortions in Random Alloys from First-Principles Theory", Phys. Rev. Lett. **87**, 156401 (2001) (See p. 30).

[55] Rowlands, D. A., Staunton, J. B., Györffy, B. L., "Korringa-Kohn-Rostoker nonlocal coherent-potential approximation", Phys. Rev. B **67**, 115109 (2003) (See p. 31).

[56] Rowlands, D. A., Ernst, A., Györffy, B. L., Staunton, J. B., "Density functional theory for disordered alloys with short-range order: Systematic inclusion of charge-correlation effects", Phys. Rev. B **73**, 165122 (2006) (See p. 31).

[57] Tomaszewicz, P., Wallwork, G. R., "Iron-aluminum alloys: A review of their oxidation behaviour", Rev. High Temp. Mater. **4**, 75 (1978) (See p. 34).

[58] Zhang, H. L., Lu, S., Punkkinen, M. P. J., Hu, Q.-M., Johansson, B., Vitos, L., "Static equation of state of bcc iron", Phys. Rev. B **82**, 132409 (2010) (See p. 35).

[59] Ruban, A., Skriver, H., Nørskov, J., "Chapter 1 - Local equilibrium properties of metallic surface alloys", in *Surface Alloys and Alloys Surfaces*, Vol. 10, edited by D. Woodruff, The Chemical Physics of Solid Surfaces (Elsevier, 2002), pp. 1–29 (See p. 36).

[60] Ropo, M., Kokko, K., Vitos, L., Kollár, J., Johansson, B., "The chemical potential in surface segregation calculations: AgPd alloys", Surface Science **600**, 904–913 (2006) (See p. 36).

[61] Ropo, M., "Ab initio study of the geometric dependence of AgPd surface segregation", Phys. Rev. B **74**, 195401 (2006) (See p. 36).

[62] Gurao, N. P., Suwas, S., "Evolution of crystallographic texture during deformation of submicron grain size titanium", English, Journal of Materials Research **26**, 523–532 (2011) (See p. 36).

UNIVERSITY OF TURKU

Painotalo Painola, Pispanristi , Finland 2019

ISBN 978-951-29-7637-9 (PRINT)
ISBN 978-951-29-7638-6 (PDF)
ISSN 0082-7002 (Print)
ISSN 2343-3175 (Online)